International Communications in Heat and Mass Transfer 35 (2008) 793–799

Contents lists available at ScienceDirect

International Communications in Heat and Mass Transfer

journal homepage: www.elsevier.com/locate/ichmt

Photographic study of pool boiling CHF from a downward-facing convex surface ☆

Alicia H. Howard, Issam Mudawar *

Boiling and Two-phase Flow Laboratory, School of Mechanical Engineering, Purdue University, West Lafayette, IN 47907, USA

ARTICLE INFO

Available online 23 April 2008

Keywords:
Critical heat flux
Pool boiling
Photographic study

ABSTRACT

Heat transfer measurements and photographic studies are performed to capture the detailed evolution of the liquid–vapor interface near critical heat flux (CHF) for a 90-degree downward-facing convex surface. The test surface, with a width of 3.2 mm and a 102.6-mm radius, consists of a series of nine heaters that dissipate equal power. Instrumentation within each heater facilitates localized heat flux and temperature measurements along the convex surface, and transparent front and back windows enable optical access to a fairly two-dimensional liquid–vapor interface. Near CHF, vapor behavior along the convex surface is cyclical, repeatedly forming a stratified vapor layer at the bottom of the convex surface, which stretches as more vapor is generated, and then flows upwards along from the surface. Subsequently, heaters at the bottom of the convex surface, followed by the other heaters, are wetted with liquid before the nucleation/coalescence/stratification/release process is repeated. This study proves that despite the pronounced thickening of the vapor layer as it propagates upwards along the convex surface, CHF always commences on the bottom of the surface.

1. Introduction

Pool boiling from the underside of downward-facing convex surfaces is important in many engineering applications. Examples include heat treating of metallic parts, handling hazardous chemical vessels during a fire, cooling electronic cables in superconductivity research, and maintaining reactor vessel integrity during a severe nuclear accident.

El-Genk and Glebov [1] examined critical heat flux (CHF) on downward-facing convex surfaces by quenching curved disks in water. They reported that CHF first occurs at the bottom of the surface and then moves radially outward as the quenching continued, causing CHF to be lowest at the heated surface edge. Cheung and Haddad [2] investigated saturated and subcooled boiling from hemispherical surfaces under both transient (quenching) and steady state conditions and, unlike El-Genk and Glebov, found CHF to be lowest at the bottom-most point of the hemisphere. They constructed an empirical localized CHF model based on the hypothesis of micro-vapor jets bursting though a liquid sublayer. However, the photographs presented by Haddad and Cheung do not substantiate the existence of the microc-vapor jets.

Most prior studies [1–4] are limited in their ability to capture the CHF mechanism, and their use of transient experiments may not produce accurate CHF data. Furthermore, useful photographic results are quite sparse, and those that are available lack clarity because of three-dimensional effects. Additionally, recommendations concerning the location of minimum CHF are sometimes inconsistent.

The key objective of the present investigation is to capture the evolution of the liquid–vapor interface near CHF for a downward-facing convex surface. An experimental apparatus is developed to facilitate (1) high-resolution photographic depiction of a two-dimensional slice of a 90-degree downward-facing convex surface, and (2) localized steady state measurements of both heat flux and surface temperature.

2. Experimental methods

Fig. 1 shows a schematic of the test apparatus. It consists of a 3.2-mm thick boiling flange that is connected to a large reservoir where the bulk fluid, Fluorinert FC-87, is stored and conditioned. The flange includes an insulative G-10 spacer as well as front and back transparent polycarbonate windows. As shown in Fig. 2(a), nine heaters are inserted along the curved portion of the G-10 spacer to create a 90-degree downward-facing convex surface with a radius of 102.6 mm. The heated surface and liquid cavity in the flange are both 3.2-mm thick, which helps restrain transverse fluid motion and render the liquid–vapor interface very discernible.

Three thermocouples measure the bulk liquid temperature within the flange. Immersion heaters in the reservoir are used to maintain the bulk fluid temperature at a subcooling of 2 °C. A water-cooled condenser coil in the reservoir recaptures most of the vapor. The

☆ Communicated by W.J. Minkowycz.

* Corresponding author.
E-mail address: mudawar@ecn.purdue.edu (I. Mudawar).

0735-1933/$ – see front matter © 2008 Elsevier Ltd. All rights reserved.
doi:10.1016/j.icheatmasstransfer.2008.03.003

Nomenclature

C_1, C_2	coefficients in one-dimensional radial conduction equation
q''	heat flux
r	radial coordinate
t	time
T	temperature
T_f	bulk liquid temperature
T_s	heater surface temperature
ΔT_{sat}	excess heater surface temperature, $T_s - T_{sat}$
ΔT_{sub}	liquid subcooling, $T_{sat} - T_f$

Greek symbol

θ	orientation angle

Subscripts

f	bulk liquid
sat	saturation

reservoir is vented to the ambient to prevent any pressure fluctuations in the system due to the vapor production.

Fig. 2(b) shows detailed dimensions of an individual heater. To construct the heaters, a plate of oxygen-free copper is turned on a lathe to form a ring with the diameters and thicknesses shown. The ring is then cut into multiple pieces such that the bulk of each copper piece is a section spanning 8.8°, except for the bottom (wetted) surface, which spans 10.0°. When the nine heaters are assembled together, as illustrated in Fig. 2(a), the heater construction minimizes circumferential heat flow between heaters while producing a continuous boiling surface. For reference purposes, the heaters are numbered sequentially from 1 (bottom-most heater) to 9 (top heater). Heat losses are minimized by sandwiching the heaters between G-10 insulation, and covering the top portions of the heaters with fiberglass batting, as illustrated in Fig. 2(c). Heat is supplied from a thick film resistor that is silver-soldered onto each copper heater. The nine heaters are powered by a single 120 V a.c. variac.

Three type-K thermocouples are embedded along the centerline of each heater at three radial distances from the wetted surface as shown in Fig. 2(b). The thermocouples are packed into 0.8-mm diameter holes with thermal grease and sealed in place with epoxy. During testing, steady state thermocouple readings are curve-fit to radial location, using the assumption of one-dimensional radial heat conduction ($T = C_1 \ln r + C_2$) to determine both the surface temperature and the heat flux. Heat flux is also calculated by dividing the power supplied by a resistor (determined from the output of current and voltage transducers) by the wetted area of the respective heater.

Prior to each test, the heater surfaces are polished lightly with a Crocus cloth and cleaned with acetone to ensure reproducible boiling results. The copper heaters as well as immersion heaters in the bulk reservoir are then turned on for about 45 min to both purge any non-condensable gases from the liquid and maintain near-saturated boiling conditions.

Both video images and still photographs are utilized to record boiling behavior at various intervals in the nucleate boiling regime as well as just prior to, and immediately following, CHF. The video images capture a temporal record of the boiling process, while the still photographs produce the higher resolution images necessary to distinguish and measure interfacial features. Video images are recorded with a Canon L1 camera, and still photographs are captured with a Nikon FM2 35 mm camera. Photographs of the entire 90-degree convex surface are taken with a 55 mm lens. Photographs of individual heater locations along the convex surface are captured with a 2X teleconverter in conjunction with a 14 mm auto-extension ring.

Uncertainty in the heat fluxes calculated from the voltage and current transducer readings is estimated at less than 0.5%; all heat flux data presented in this paper are therefore based on the transducer measurements. The uncertainty in surface temperature using this heat flux and the aforementioned curve fitting procedure ranges from 1.7 to 2.6 °C. Heat loss through the insulation is estimated at less than 5% of the measured electrical heat input.

3. Experimental results

3.1. Nucleate boiling and CHF measurements

Fig. 3 shows boiling curves for the nine heaters forming the 90-degree downward-facing convex surface. The downward-facing portion of the convex surface inhibits natural convection around heaters 1 and 2, inciting boiling at a superheat temperature of $\Delta T_{sat} < 2$ °C, rather than the typical 10 °C value for upward-facing surfaces in Fluorinerts [5]. Boiling commences on the lowest heaters (1 and 2) and then propagates up the convex surface. The nucleate boiling regime is similar for all nine heaters. The unsteady rise in surface temperature associated with CHF occurs at heaters 1 and 2 first, followed by the other heaters.

It is clear from Fig. 3 that heater 9 is the coolest for any heat flux, while heater 1 is the hottest, followed by heater 2. As the heat flux is increased, the degradation in heat transfer from heaters 1 and 2 becomes more pronounced. This is believed to be the result of vapor stratification on these two lower heaters, contrasted with the additional cooling available to heaters 3 through 9 from the buoyancy-driven liquid–vapor flow along the convex surface.

Stable heat fluxes approximately equal to 95% of CHF are hereafter denoted as CHF−, and heat fluxes slightly greater than CHF as CHF+. Fig. 3(b) shows the transient progression of the temperature excursion. Notice that none of the heaters detect an immediate rapid temperature rise following a power increment from CHF−. However, once initiated, the temperature rise at CHF+ is almost twice as large as at CHF−. At approximately 2 min into CHF+, a sharp increase in the temperature-time gradient ensues for heaters 1 and 2. Since these two heaters are essentially insulated with vapor, heat starts to “leak” into heater 3, causing the temperature gradient of heater 3 to increase as well. Within 5 min, heaters 3 and 4 begin experiencing a sharp temperature rise. At approximately 5.5 min, heater 1 is turned off by the data acquisition system, but the experiment is allowed to continue for another minute so that the temperature excursions in heaters 2 through 4 could be further observed. It is speculated that had the test been allowed to continue, all remaining heaters would have eventually experienced a similar rapid temperature rise. The transient data in Fig. 3(a) reveal CHF is triggered at the most downward-facing heaters (1 and 2) and then propagates up the convex surface.

3.2. Flow visualization results

To gain further insight into the CHF mechanism, both still and video photography are used to record boiling phenomena at various intervals in the nucleate boiling region as well as just prior to and immediately following CHF.

Figs. 4–6 show still photographs of the liquid–vapor interface on the convex surface for different conditions. Because the test apparatus is backlit, the heater surface appears as a black quarter-circle. The reference grid, measurement scale, and heater numbers are affixed to the back polycarbonate plastic window of the test flange and are visible in all the photos. Grid lines denoting radial position are spaced in 1-cm increments, while those denoting angular position are spaced 10° apart, corresponding to individual heater locations.

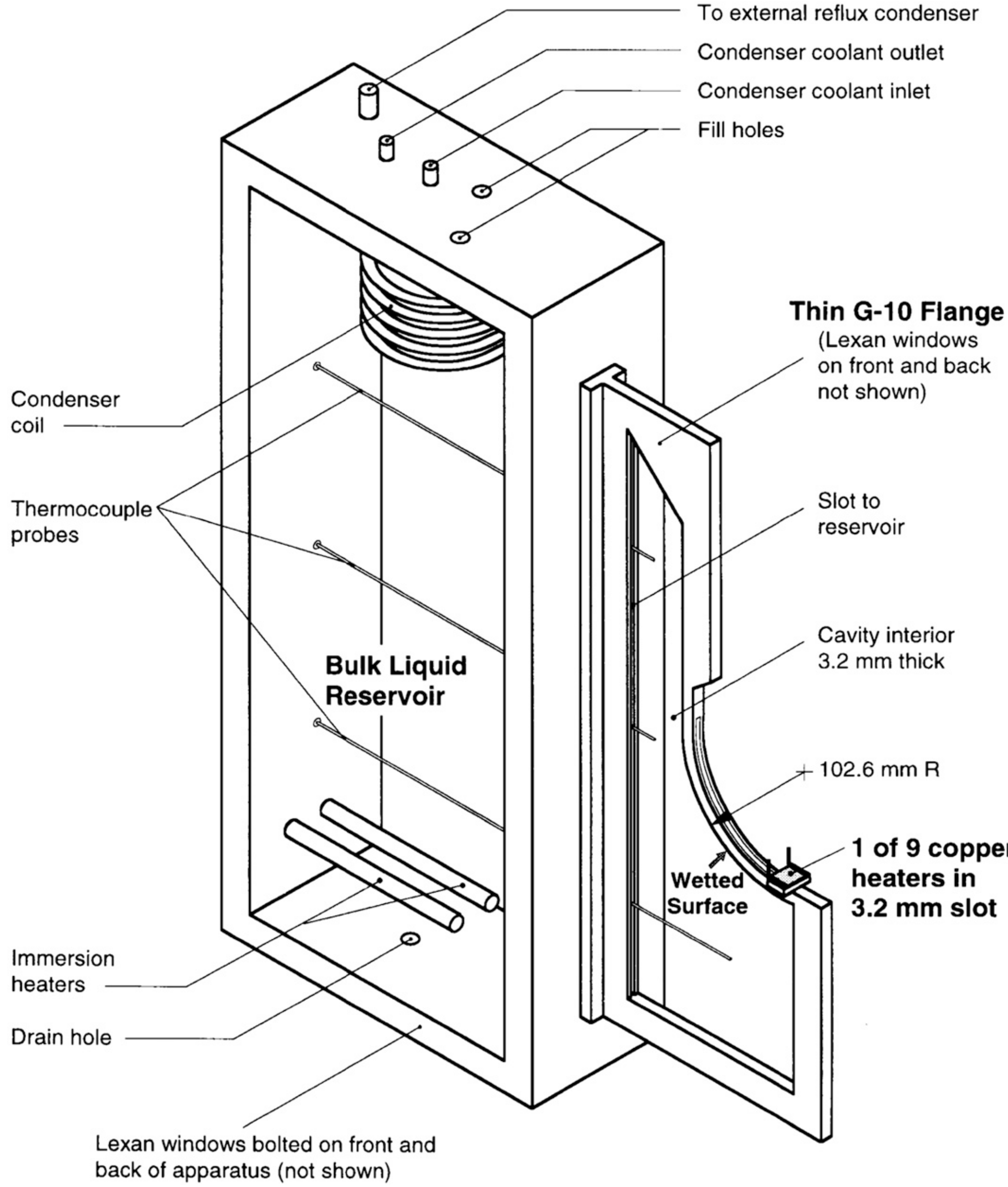

Fig. 1. Test apparatus for pool boiling from downward-facing convex surface.

As discussed earlier, boiling commences on the bottom heaters (1 and 2). As the individual bubbles traverse the heated surface, they accumulate additional vapor, causing them to grow in size and form oblong bubbles. At incipience, the oblong bubbles are small and separated by large segments of liquid. As the heat flux is increased, these bubbles grow longer and the length of the liquid segment between bubbles shorter. Fig. 4 shows a photo of the convex surface at 25% of CHF. The photo is representative of what is observed in video images for low heat flux conditions. Clearly shown is a wavy liquid–vapor interfacial behavior reminiscent of observations by Howard and Mudawar [5,6] for pool boiling CHF at different orientations, as well as by Galloway and Mudawar [7] and Sturgis and Mudawar [8] for flow boiling CHF.

At heat fluxes above 75% of CHF, the boiling process becomes cyclical in nature. The period of the cycle does not increase or decrease with increasing heat flux. Instead it remains fairly constant at 0.12 s per cycle, even during CHF+. Because of this cyclical behavior, high heat flux pool boiling on the convex surface cannot be accurately represented by a single photo. Figs. 5 and 6 show two series of five photographs taken at CHF− for the full convex surface and the two bottom heaters, respectively. Even though the photos in the two figures are taken at different times, they depict equivalent phases of a single boiling cycle; the top photo in each figure represents the beginning of a cycle and the bottom photo the end. Because of the large span of the convex surface, different boiling patterns occur simultaneously on different portions of the surface during a single cycle. The following is a description of the boiling cycle starting at heaters 1 and 2:

(a) First, liquid wets the bottom heaters (1 and 2), and discrete bubbles are formed.
(b) As the bubbles grow in volume, they begin to coalesce into a vapor layer on the bottom heaters.
(c) The vapor layer engulfs heaters 1 and 2 and grows in length to cover an increasing fraction of the convex surface area.
(d) The vapor layer on heaters 1 and 2 thins out as the vapor travels away from these heaters. The vapor layer grows shorter and thicker as it travels upwards along the convex surface.

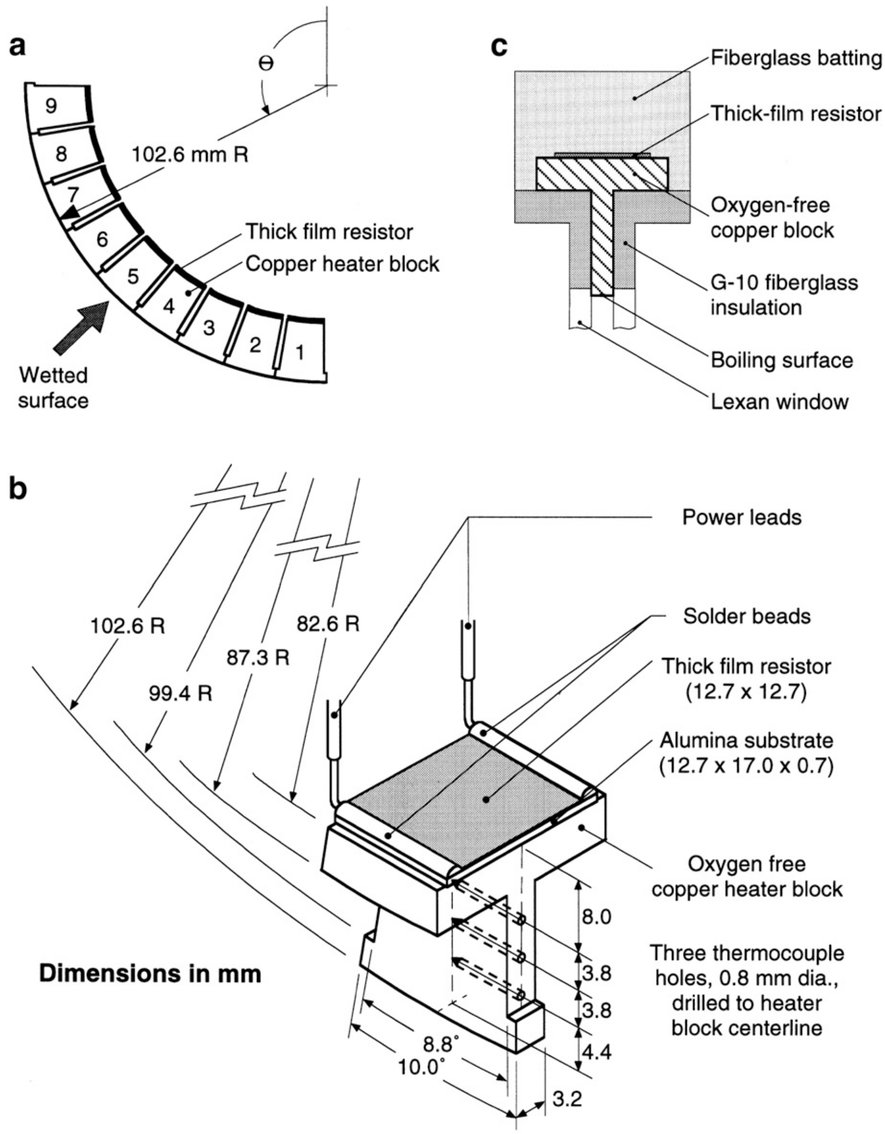

Fig. 2. (a) Arrangement of heaters along downward-facing convex surface. (b) Single heater details. (c) Heater insulation.

(e) The bottom heaters and, subsequently, the other heaters, are wetted with liquid for a brief period before the boiling nucleation/coalescence/stratification/release process is repeated.

Photographs at 75% of CHF (not shown here) are very similar to those in Figs. 5 and 6 for CHF−, except that a thin sublayer of liquid is sometimes observed within the vapor wave for the lower heat flux. This liquid sublayer is not observed in photos taken at 90% of CHF or higher, as shown in Figs. 5 and 6, proving the liquid sublayer had dried out for the most part.

Howard and Mudawar [5] noted that at high heat flux conditions leading to CHF, vapor behavior on a flat downward-facing surface experiencing pool boiling is categorically different from that for all other surface orientations. In the *downward-facing CHF region* observed by Howard and Mudawar, which ranges from 165° to 180°, vapor bubbles grow and coalesce together, eventually covering most of the heater surface. As the vapor layer continues to grow, it reaches an edge where the vapor is released by buoyancy. Liquid is then able to wet the heater surface, causing a revival of bubble nucleation and initiating a new nucleation/coalescence/stratification/release cycle. This is very similar to the vapor behavior observed on the convex surface. Additionally, heaters 1 and 2, where CHF commences on the convex surface, have equivalent orientations of 160° to 180°, which are comparable with the orientation range of the downward-facing CHF region (165° to 180°) observed and predicted by Howard and Mudawar for FC-72 on a flat inclined surface.

4. Conclusions

Near-saturated pool boiling experiments and flow visualization studies were performed on a 90-degree slice of a downward-facing convex surface to explore liquid–vapor interfacial behavior near CHF. Key conclusions from the study are as follows:

(1) Boiling commences on the bottom heaters (1 and 2), and then propagates up the convex surface. Nucleate boiling occurs with excess temperatures much smaller than those experienced on upward-facing flat surfaces.
(2) The orientations of the bottom heaters (1 and 2) inhibit natural convection, while the buoyancy-driven liquid–vapor flow along the convex surface increases heat transfer from the other heaters (3 through 9). This causes the temperatures of the bottom heaters to be higher than all other heaters, regardless of heat flux. As the heat flux increases, cooling deficiencies of the bottom heaters become even more pronounced.

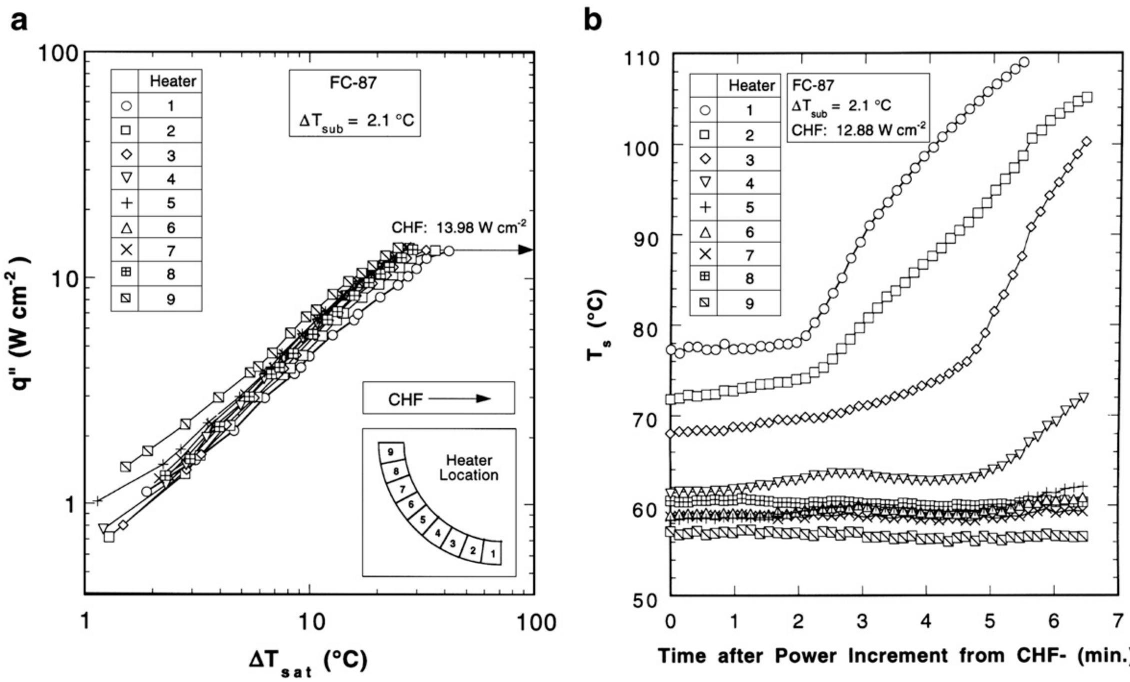

Fig. 3. (a) Local boiling curves for nine heaters. (b) Transient heater temperatures following CHF.

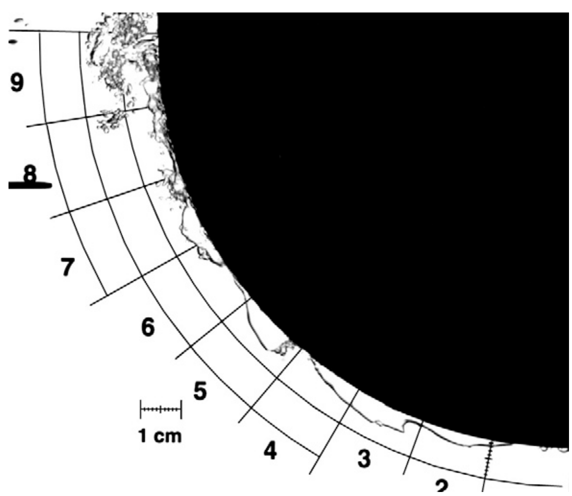

Fig. 4. Vapor layer along downward-facing convex surface at 25% of CHF.

(3) Near CHF, the boiling is cyclical in nature. Individual bubbles nucleate, grow, and coalesce together, forming a vapor layer that essentially insulates the heaters for brief periods of time. As the vapor layer departs, the bottom heaters, followed by the other heaters, are wetted with liquid before the nucleation/coalescence/stratification/release process is repeated. This boiling cycle is similar to the cycle previously observed by the authors near CHF on flat downward-facing heaters.

(4) CHF commences on the bottom heaters (1 and 2), which have equivalent orientations of 160° to 180°. These orientations are comparable with the orientation range of the *downward-facing CHF region* observed and predicted by Howard and Mudawar [5] for flat downward-facing heaters.

References

[1] M.S. El-Genk, A.G. Glebov, Transient pool boiling from downward-facing curved surfaces, Int. J. Heat Mass Transfer 38 (1995) 2209–2224.
[2] F.B. Cheung, K.H. Haddad, A hydrodynamic critical heat flux model for saturated pool boiling on a downward facing curved heating surface, Int. J. Heat Mass Transfer 40 (1997) 1291–1302.
[3] T.Y. Chu, B.L. Bainbridge, R.B. Simpson, J.H. Bentz, Ex-vessel boiling experiments: laboratory and reactor scale testing of the flooded cavity concept for in-vessel core retention—Part I: observations of quenching of downward-facing surfaces, Nucl. Eng. Des. 169 (1977) 77–88.
[4] T.G. Theofanous, S. Syri, T. Salmassi, O. Kymalainen, H. Tuomisto, Critical heat flux through curved, downward facing thick walls, Nucl. Eng. Des. 151 (1994) 247–258.
[5] A.H. Howard, I. Mudawar, Orientation effects on pool boiling critical heat flux (CHF) and modeling of CHF for near-vertical surfaces, Int. J. Heat Mass Transfer 42 (1999) 1665–1688.
[6] I. Mudawar, A.H. Howard, C.O. Gersey, An analytical model for near-saturated pool boiling CHF on vertical surfaces, Int. J. Heat Mass Transfer 40 (1997) 2327–2339.
[7] J.E. Galloway, I. Mudawar, CHF mechanism in flow boiling from a short heated wall—I. Examination of near-wall conditions with the aid of photomicrography and high speed video imaging, Int. J. Heat Mass Transfer 36 (1993) 2511–2526.
[8] J.C. Sturgis, I. Mudawar, Critical heat flux in a long, rectangular channel subjected to one-sided heating—I. Flow visualization, Int. J. Heat Mass Transfer 42 (1999) 1835–1847.

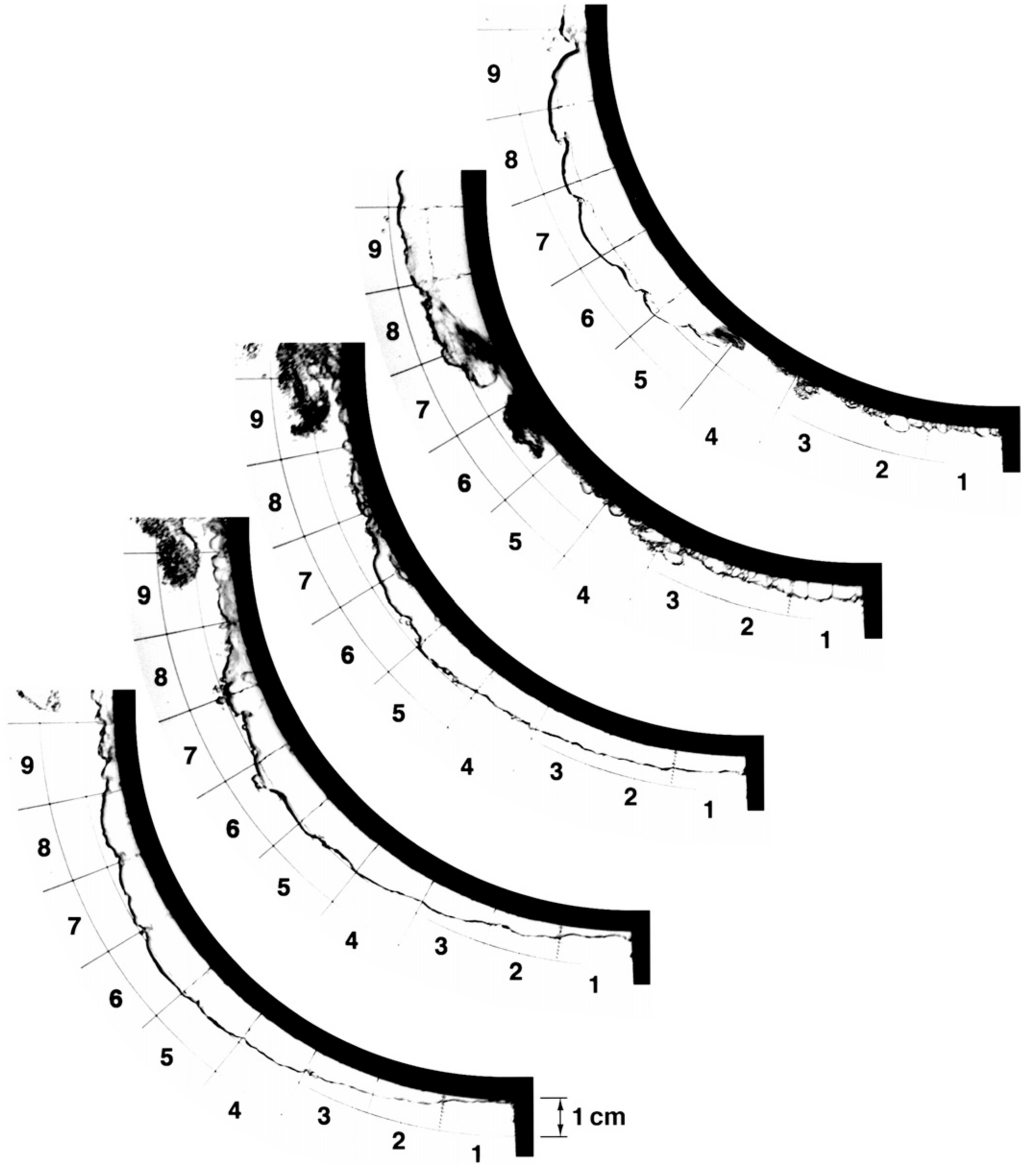

Fig. 5. Development of vapor layer along downward-facing convex surface at CHF−.

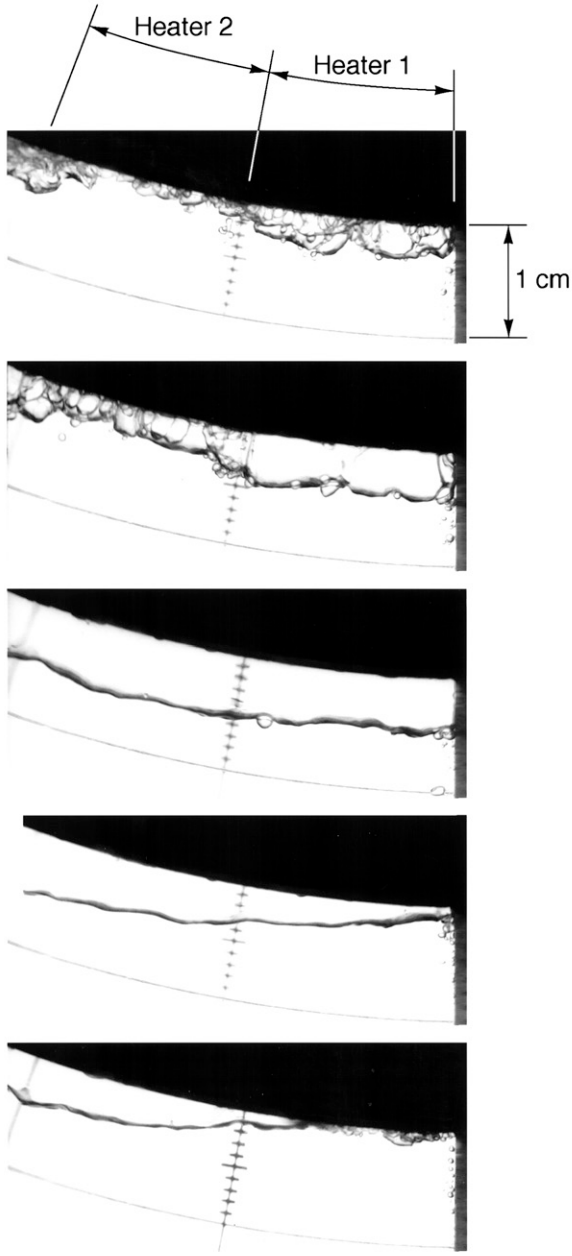

Fig. 6. Development of vapor layer for heaters 1 and 2 at CHF−.